



Short communication

## Synthesis of lithium insertion material $\text{Li}_4\text{Ti}_5\text{O}_{12}$ from rutile $\text{TiO}_2$ via surface activation

Tao Yuan, Rui Cai, Peng Gu, Zongping Shao\*

State Key Laboratory of Materials-Oriented Chemical Engineering, College of Chemistry & Chemical Engineering, Nanjing University of Technology, No. 5 Xin Mofan Road, Nanjing 210009, PR China

## ARTICLE INFO

## Article history:

Received 16 June 2009

Received in revised form

16 November 2009

Accepted 18 November 2009

Available online 24 November 2009

## Keywords:

Lithium titanate

Rutile titanium dioxide

Cellulose

Anode material

Rate capacity

## ABSTRACT

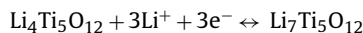
The synthesis of spinel-type lithium titanate,  $\text{Li}_4\text{Ti}_5\text{O}_{12}$ , a promising anode material of secondary lithium-ion battery, from “inert” rutile  $\text{TiO}_2$ , is investigated. On the purpose of increasing the reactivity of rutile  $\text{TiO}_2$ , it is treated by concentrated  $\text{HNO}_3$ . By applying such activated rutile  $\text{TiO}_2$  as the titanium source in combination with the cellulose-assisted combustion synthesis, phase-pure  $\text{Li}_4\text{Ti}_5\text{O}_{12}$  is successfully synthesized at  $800^\circ\text{C}$ , at least  $150^\circ\text{C}$  lower than that based on solid-state reaction. The resulted oxide shows a reversible discharge capacity of  $\sim 175\text{mAh g}^{-1}$  at 1 C rate, near the theoretical value. The resulted oxide also shows promising high rate performance with a discharge capacity of  $\sim 100\text{mAh g}^{-1}$  at 10 C rate and high cycling stability.

© 2009 Elsevier B.V. All rights reserved.

## 1. Introduction

Graphite/carbon-related materials have been the most applied anodes in small size secondary lithium-ion batteries as power source of personal electronics, such as laptops, camcorders and digital cameras [1–3]. For larger size applications like electric vehicles and dispersed energy storage systems where high rate charge/discharge is frequently required, the carbon anode may suffer from serious safety problems. Due to the low lithium intercalating voltage of approximately 100 mV (vs.  $\text{Li/Li}^+$ ), highly reactive metallic lithium forms easily under fast charge rate [4], which may deposit on the surface of electrode particles and has the high risk to react with the electrolyte or highly charged cathodes to result in combustion or explosion.

Recently lithium insertion oxides like  $\text{Li}_4\text{Ti}_5\text{O}_{12}$  have acquired considerable attention as alternative anode to carbon/graphite in rechargeable lithium-ion batteries [5–9]. It is a spinel-type composite oxide allowing the reversible lithium insertion at room temperature via the reaction as follows:



Three lithium can insert into the lattice of  $\text{Li}_4\text{Ti}_5\text{O}_{12}$  molecule with the formation of  $\text{Li}_7\text{Ti}_5\text{O}_{12}$ , resulting in a theoretical capacity

of  $175\text{mAh g}^{-1}$ . During the insertion process, the phase structure of the oxide changes from a spinel-type ( $\text{Li}_4\text{Ti}_5\text{O}_{12}$ ) to a rock-salt type ( $\text{Li}_7\text{Ti}_5\text{O}_{12}$ ) [10], both structures have the same cubic lattice symmetry and a cell volume difference less than 0.1% [11]. Thereby,  $\text{Li}_4\text{Ti}_5\text{O}_{12}$  is also named as a zero-strain lithium insertion material [11]. This is a beneficial feature ensuring a long cycling life. Similar to  $\text{LiFePO}_4$  cathode, the two-phase mechanism for the lithium intercalation/de-intercalation results in an extremely flat discharge platform at around 1.55 V for  $\text{Li}_4\text{Ti}_5\text{O}_{12}$ . Such a medium discharge voltage is well above the formation potential of metallic lithium; as a result, the safety problem associated with carbon-based anode due to metallic formation during fast charge is effectively avoided by adopting the  $\text{Li}_4\text{Ti}_5\text{O}_{12}$  anode. Although its medium level of discharge voltage discourages the application as a positive electrode, it can be coupled with a high-voltage electrode such as 4 V  $\text{LiMn}_2\text{O}_4$  and  $\text{LiCoO}_2$  or 5 V  $\text{LiCoPO}_4$  to provide a cell with an operating voltage of 2.5–3.5 V [12].

One practical problem associated with coarse  $\text{Li}_4\text{Ti}_5\text{O}_{12}$  anode is its poor rate performance because of its negligible electronic conductivity. Surface coating with conductive material such as amorphous carbon and reducing the grain size are the effective ways to minimize the electrode polarization resistance at high charge/discharge rate [13–17]. The decrease of grain size would not only lessen the diffusion distance for electron and lithium ion but also increase the surface area for interfacial reaction; consequently the rate performance can be effectively improved [15–17]. Consequently, the preparation of ultrafine  $\text{Li}_4\text{Ti}_5\text{O}_{12}$  powder becomes one of the key steps towards the commercialization of  $\text{Li}_4\text{Ti}_5\text{O}_{12}$

\* Corresponding author. Tel.: +86 25 83172256; fax: +86 25 83172256.  
E-mail address: [shaozp@njut.edu.cn](mailto:shaozp@njut.edu.cn) (Z. Shao).

anode in rechargeable lithium-ion batteries. Although nano-sized  $\text{Li}_4\text{Ti}_5\text{O}_{12}$  has been successfully prepared in the literature using advanced techniques such as sol-gel process [18–21], up to now, the most attractive process for potential industrial application is still the solid-state reaction by applying cheap and abundant  $\text{TiO}_2$  as the titanium source for lower costs.

It is well known that the rutile  $\text{TiO}_2$  is the most suitable raw material for synthesis of  $\text{Li}_4\text{Ti}_5\text{O}_{12}$  from the aspect of material availability, although the anatase  $\text{TiO}_2$  can accommodate much more lithium in its crystal lattice compared to rutile  $\text{TiO}_2$  [22–24]. In fact most of these studies reported that bulk rutile hardly inserts any lithium at room temperature. Consequently, very high calcination temperature is needed to facilitate the solid-state reaction between rutile  $\text{TiO}_2$  and  $\text{Li}_2\text{CO}_3/\text{LiOH}$  to form  $\text{Li}_4\text{Ti}_5\text{O}_{12}$  [25,26]. The high-temperature calcination, however, results in not only the difficulty in precise control of the cation stoichiometry, but also the serious sintering of the product, consequently, poor rate performance is frequently observed for the as-prepared sample.

Previously we successfully prepared high rate performance  $\text{Li}_4\text{Ti}_5\text{O}_{12}$  oxide at reduced temperature via a cellulose-assisted combustion technique adopting anatase  $\text{TiO}_2$  as the titanium source [27]. In this study, we reported the synthesis of  $\text{Li}_4\text{Ti}_5\text{O}_{12}$  from more commercially available but more passive rutile  $\text{TiO}_2$  at reduced temperature. A treatment of rutile  $\text{TiO}_2$  by concentrated nitric acid significantly improved the reaction kinetics, consequently, a calcination temperature as low as  $800^\circ\text{C}$  is sufficient to obtain a phase-pure  $\text{Li}_4\text{Ti}_5\text{O}_{12}$  by adopting the cellulose-assisted combustion technique. The resulted anode material shows high rate performance and high cycling stability.

## 2. Experimental

### 2.1. Powder synthesis

The  $\text{Li}_4\text{Ti}_5\text{O}_{12}$  oxides were synthesized by a cellulose-assisted combustion process adopting rutile  $\text{TiO}_2$  as titanium source with excess 2 wt.% Li to compensate for the loss of Li followed by high-temperature calcination [27]. Cotton fiber, pre-activated by  $\text{HNO}_3$ , was applied as the cellulose. Commercial  $\text{TiO}_2$  rutile powder with a surface area of  $33.2\text{ m}^2\text{ g}^{-1}$ , purchased from Hangzhou WAN JING New Material Co., Ltd. (China), is adopted as the titanium source. It is either applied directly as received or pretreated by concentrated  $\text{HNO}_3$  (67%) at room temperature for 10 h. For comparison,  $\text{Li}_4\text{Ti}_5\text{O}_{12}$  oxide was also synthesized by solid-state reaction adopting  $\text{Li}_2\text{CO}_3$  and rutile  $\text{TiO}_2$  as the raw materials.

### 2.2. Electrode fabrication

The electrochemical performance of  $\text{Li}_4\text{Ti}_5\text{O}_{12}$  powders was carried out with coin-shape cells using metallic lithium film as the counter and reference electrode at room temperature ( $\sim 30^\circ\text{C}$ ). The cells are based on the configuration of Li metal (–) |electrolyte|  $\text{Li}_4\text{Ti}_5\text{O}_{12}$  (+) with a liquid electrolyte (1 M solution of  $\text{LiPF}_6$  in ethylene carbonate (EC)–dimethyl carbonate (DMC) (1:1, v/v)). Microporous polypropylene film (Celgard 2400) was used as the separator. 85 wt.%  $\text{Li}_4\text{Ti}_5\text{O}_{12}$  with 8 wt.% conductive Super P (NCM HERSBIT Chemical Co., Ltd., China) and 7 wt.% polyvinylidene fluoride (PVDF) binder homogeneously mixed in N-methyl pyrrolidinone (NMP) were prepared into viscous slurries for efficient deposition. The slurries were deposited on current collectors of copper foil ( $10\ \mu\text{m}$ ) by blade, which was pretreated by etching with 1 M nitric acid solutions followed by rinsing with water and then acetone. The electrode was then dried under vacuum at  $100^\circ\text{C}$  for 12 h before electrochemical evaluation. Cell assembly was conducted in a glove box filled with pure argon.

### 2.3. Characterization

The crystal structures of the synthesized powders were examined by X-ray diffraction (XRD) using a Bruker D8 advance diffractometer with filtered  $\text{Cu K}\alpha$  radiation. The experimental diffraction patterns were collected at room temperature by step scanning in the range of  $10^\circ \leq 2\theta \leq 80^\circ$ . The specific surface area of the samples was characterized by  $\text{N}_2$  adsorption at the temperature of liquid nitrogen using a BELSORP II instrument. Prior to analysis, the samples were treated at  $100^\circ\text{C}$  for 3–5 h in vacuum to remove the surface adsorbed species.

The charge–discharge characteristics of the cells were recorded over the potential range between 1.0 and 3.0 V using a NEWARE BTS-5V50 mA computer-controlled battery test station at different rates of 1–40 C at  $30^\circ\text{C}$ .

## 3. Results and discussion

### 3.1. Synthesis

The synthesis of  $\text{Li}_4\text{Ti}_5\text{O}_{12}$  by traditional solid-state reaction applying rutile  $\text{TiO}_2$  as reactant was first investigated. Stoichiometric amounts of  $\text{Li}_2\text{CO}_3$  and rutile  $\text{TiO}_2$  (as received) were well mixed by high energy ball milling (Fritsch, Pulveriette 6) at a rotation speed of 400 rpm for 2 h, the mixture was then submitted for calcination at various temperatures in air for a selected time (5–24 h). Fig. 1a shows the corresponding room temperature X-ray diffraction patterns of the powders calcined at  $800$ – $950^\circ\text{C}$ . After the calcination at  $800^\circ\text{C}$  for 5 h, there was still considerable amount of rutile  $\text{TiO}_2$  detected in the product by XRD. With the increase of calcination temperature and dwell time, the relative intensity of the spinel phase increased. However, minor amount of rutile  $\text{TiO}_2$  was still detected even after the calcination at  $950^\circ\text{C}$  for 24 h. In the literature, time-consuming intermitting grinding is needed to promote the solid-state reaction by breaking up the particle size and making intimating contact of the reactants to obtain pure phase  $\text{Li}_4\text{Ti}_5\text{O}_{12}$  [28].

In our previous paper, we have demonstrated that the cellulose-assisted method can result in the reduced synthesis temperature of phase-pure  $\text{Li}_4\text{Ti}_5\text{O}_{12}$  when adopting anatase  $\text{TiO}_2$  as the titanium source. The cellulose can suppress the grain growth of anatase  $\text{TiO}_2$  during the calcination on the one hand; the combustion process created instant high temperature to promote the phase reaction on the other hand. Consequently, nanocrystalline phase-pure  $\text{Li}_4\text{Ti}_5\text{O}_{12}$  was obtained at a low calcination temperature of  $750^\circ\text{C}$  [27]. The same technique was also adopted in this study on the purpose to reduce the synthesis temperature of  $\text{Li}_4\text{Ti}_5\text{O}_{12}$  from rutile  $\text{TiO}_2$ . The sequence of materials addition was found to have significant effect on the phase formation with the optimal sequence of first impregnating the cellulose with a mixed solution of  $\text{LiNO}_3$  and glycine, then with a suspension of  $\text{TiO}_2$  and  $\text{HNO}_3$  [27]. The same sequence was adopted for the synthesis of  $\text{Li}_4\text{Ti}_5\text{O}_{12}$  from rutile  $\text{TiO}_2$ . Flame combustion was suddenly happened when the dried precursors were quickly heated up by an electrical oven at  $250^\circ\text{C}$ , the combustion last for tens of seconds and left a primary product which took the morphology of the initial cellulose fiber. It was then pulverized and submitted for phase examination. Fig. 1b shows the XRD patterns of the primary product and that by further calcination at various temperatures for 5 h in air. After the calcination at  $800^\circ\text{C}$  for 5 h, the rutile  $\text{TiO}_2$  phase was still significant in the product based on the XRD results, although the relative intensity of spinel to rutile is several times that of the product calcined at the same temperature from the solid-state reaction. When the solid precursor was calcined at  $850^\circ\text{C}$  for 5 h, the main spinel phase was formed and the diffraction peaks of rutile  $\text{TiO}_2$

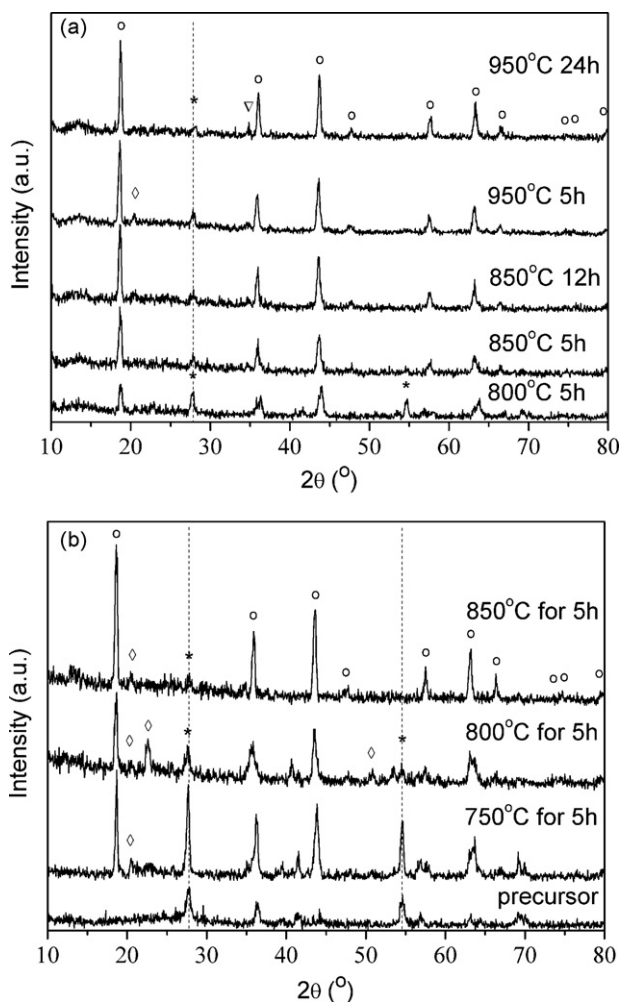


**Fig. 1.** XRD patterns of  $\text{Li}_4\text{Ti}_5\text{O}_{12}$ : (a) the pristine rutile  $\text{TiO}_2$  as reactant prepared by solid-state reaction and (b) pristine rutile  $\text{TiO}_2$  as reactant prepared by cellulose-assisted combustion and further calcined at different temperatures for 5 h. (o) Spinel  $\text{Li}_4\text{Ti}_5\text{O}_{12}$ , (\*) rutile  $\text{TiO}_2$ , (◇)  $\text{Li}_2\text{TiO}_3$ , and (▽)  $\text{Ti}_2\text{O}_3$ .

phase were in very weak intensity. It suggests that a calcination temperature around  $850^\circ\text{C}$  is needed by applying the cellulose-assisted combustion technique when adopting rutile  $\text{TiO}_2$  as the reactant.

To reduce the synthesis temperature of  $\text{Li}_4\text{Ti}_5\text{O}_{12}$  via the cellulose-assisted combustion technique, the rutile  $\text{TiO}_2$  was activated by  $\text{HNO}_3$  treatment at room temperature for 12 h. It was observed that the combustion behavior of the solid precursor is similar whether the rutile  $\text{TiO}_2$  was acid treated or not. Fig. 2 shows the XRD patterns of the primary product prepared from the cellulose-assisted combustion technique by adopting the acid treated rutile  $\text{TiO}_2$  as the titanium source and the samples after the further calcination at various temperatures for 5 h. The spinel phase, although in very weak intensity, started to appear in the primary product after the auto-combustion. After the further calcination at  $750^\circ\text{C}$  for 5 h, the oxide displayed the main spinel phase together with weak rutile  $\text{TiO}_2$  phase and  $\text{Li}_2\text{TiO}_3$  phase. When the calcination temperature elevated to  $800^\circ\text{C}$ , the  $\text{TiO}_2$  phase was totally disappeared and a phase-pure spinel oxide was observed. It suggests that the  $\text{Li}_4\text{Ti}_5\text{O}_{12}$  phase was successfully formed at around  $800^\circ\text{C}$ . Compared to the results in Fig. 1, the synthesis temperature of a phase-pure  $\text{Li}_4\text{Ti}_5\text{O}_{12}$  was effectively lowered.

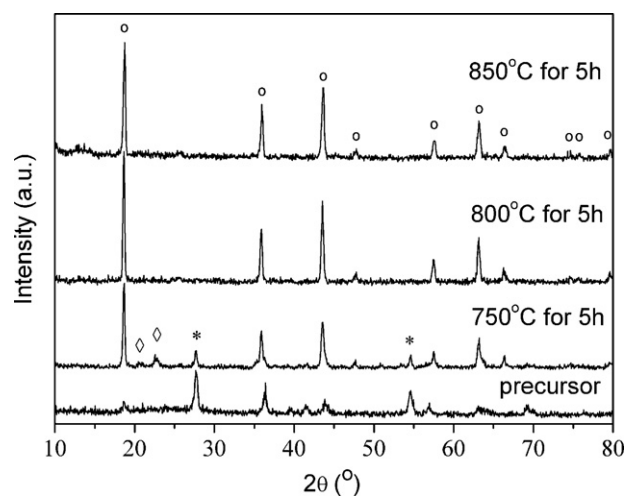


**Fig. 2.** X-ray diffraction patterns of the primary product and the samples after the further calcination at various temperatures for 5 h, prepared from the cellulose-assisted combustion technique by adopting the acid treated rutile  $\text{TiO}_2$  as the titanium source. (o) Spinel  $\text{Li}_4\text{Ti}_5\text{O}_{12}$ , (\*) rutile  $\text{TiO}_2$ , and (◇)  $\text{Li}_2\text{TiO}_3$ .

### 3.2. Electrochemical performance

The electrochemical performance of the various  $\text{Li}_4\text{Ti}_5\text{O}_{12}$  oxides was then investigated at room temperature. Shown in Fig. 3 are the second discharge curves at various discharge rates of the  $\text{Li}_4\text{Ti}_5\text{O}_{12}$  anodes synthesized from rutile  $\text{TiO}_2$  by solid-state reaction after the calcination at  $950^\circ\text{C}$  for 24 h (Fig. 3a), from the cellulose-assisted combustion technique applying rutile  $\text{TiO}_2$  as titanium source after the calcination at  $850^\circ\text{C}$  for 5 h (Fig. 3b), and from the cellulose-assisted combustion synthesis applying the acid treated rutile  $\text{TiO}_2$  as the titanium source and after the calcination at  $800^\circ\text{C}$  for 5 h (Fig. 3c). For the sample from the solid-state reaction, a discharge capacity of only  $86\text{mAh g}^{-1}$  was obtained at 1 C rate, much lower than the theoretic value of  $\sim 175\text{mAh g}^{-1}$ . Furthermore, the capacity in the flat plateau was only about  $35\text{mAh g}^{-1}$ . With the increase of discharge rate the capacity decreased sharply, it retained only  $40\text{mAh g}^{-1}$  at 5 C rate. These results are much worse than that prepared by a sol-gel process, or by the cellulose-assisted combustion process by adopting anatase  $\text{TiO}_2$  as the titanium source [19,27]. Two possible explanations for such poor performance are as follows. First there was still some minor impurity phase presented in the sample prepared from the solid-state reaction after the calcination at  $950^\circ\text{C}$  for 24 h, suggesting the actual composition of the anode may deviate from the nominal composition of  $\text{Li}_4\text{Ti}_5\text{O}_{12}$ ; second such high calcination temperature ( $950^\circ\text{C}$ ) and prolonged calcination time led to the serious grain growth and the decrease of surface area. Kavan et al. studied the surface area and trace impurities on the electrochemical properties of  $\text{Li}_4\text{Ti}_5\text{O}_{12}$  systematically [29]. Both resulted in a large polarization resistance for the lithium insertion into and extraction from the lattice. For the sample prepared from the cellulose-assisted combustion technique adopting rutile  $\text{TiO}_2$  as reactant, much better discharge performance was obtained. A pretty flat discharge platform was observed at around 1.55 V at 1 C rate, in well agreement with the two-phase mechanism for the charge/discharge of  $\text{Li}_4\text{Ti}_5\text{O}_{12}$  anode. The reversible discharge capacity of 117, 104, 87, 62, 44 and  $32\text{mAh g}^{-1}$  was observed at a discharge rate of 1, 2, 5, 10, 20 and 40 C, respectively. When adopting acid treated rutile as the raw material of titanium, a discharge capacity of 175, 140, 115, 92, 71, and  $56\text{mAh g}^{-1}$  was obtained at 1, 2, 5, 10, 20, and 40 C discharge rates, respectively. It suggests that the acid treatment greatly improved the rate performance of  $\text{Li}_4\text{Ti}_5\text{O}_{12}$  as compared to that adopting rutile  $\text{TiO}_2$  by the same cellulose-assisted combus-

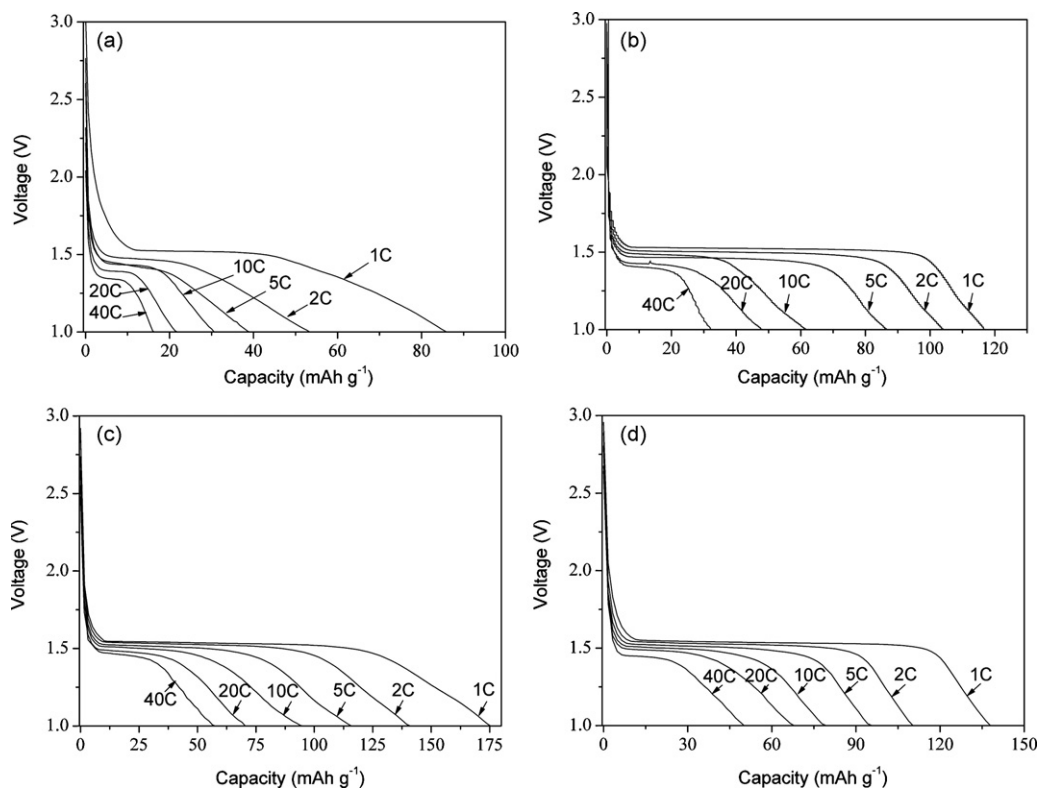


**Fig. 3.** The discharge profiles of the  $\text{Li}_4\text{Ti}_5\text{O}_{12}$  oxides from 1 to 3 V at different rates, prepared by (a) solid-state reaction calcined at  $950^\circ\text{C}$  for 24 h with rutile  $\text{TiO}_2$  as reactant; (b) cellulose-assisted combustion process and further calcined at  $850^\circ\text{C}$  for 5 h with rutile  $\text{TiO}_2$  as reactant; (c) and (d) cellulose-assisted combustion process and further calcined at 800 and  $850^\circ\text{C}$  for 5 h, respectively, with  $\text{HNO}_3$ -treated rutile  $\text{TiO}_2$  as reactant.

tion synthesis. The performance of  $\text{Li}_4\text{Ti}_5\text{O}_{12}$  is closely related with the grain size of the oxide. The surface area of  $\text{Li}_4\text{Ti}_5\text{O}_{12}$  with rutile  $\text{TiO}_2$  and acid treated rutile  $\text{TiO}_2$  as the titanium source during the combustion synthesis is  $1.09\text{ m}^2\text{ g}^{-1}$  ( $850^\circ\text{C}$ ) and  $2.78\text{ m}^2\text{ g}^{-1}$  ( $800^\circ\text{C}$  calcined), respectively. The improved  $\text{Li}_4\text{Ti}_5\text{O}_{12}$  anode performance from the acid treated rutile  $\text{TiO}_2$  raw material is likely associated with the increased surface area and accessible active area due to the reduced calcination temperature for obtaining pure phase  $\text{Li}_4\text{Ti}_5\text{O}_{12}$  [29]. To support such assumption, the rate performance of  $\text{Li}_4\text{Ti}_5\text{O}_{12}$  prepared by the cellulose-assisted combustion synthesis applying the acid treated rutile  $\text{TiO}_2$  as titanium source and calcined at  $850^\circ\text{C}$  was also conducted. As shown in Fig. 3d, a

reversible discharge capacity of  $137, 108, 94, 77, 63,$  and  $49\text{ mAh g}^{-1}$  was observed at 1, 2, 5, 10, 20 and  $40\text{ C}$ , much lower than that calcined at  $800^\circ\text{C}$ , and only slightly improved as compared to that calcined at the same temperature with rutile  $\text{TiO}_2$  as the raw material during the combustion synthesis. The surface area of the  $850^\circ\text{C}$  calcined sample is  $1.32\text{ m}^2\text{ g}^{-1}$ , similar to that prepared from rutile  $\text{TiO}_2$  and calcined at the same temperature ( $1.09\text{ m}^2\text{ g}^{-1}$ ).

The cycling stability of the  $800^\circ\text{C}$  calcined  $\text{Li}_4\text{Ti}_5\text{O}_{12}$  prepared from cellulose-assisted combustion synthesis adopting acid treated  $\text{TiO}_2$  is shown in Fig. 4. High cycling stability was observed. At 1, 2, 5, 10, 20 and  $40\text{ C}$  rates, the decay in discharge capacity after the 51 cycles was only 9.7, 9.1, 9.9, 6.1, 2.1 and 2.6%, respectively. It suggests the high reversibility and stability of the Li-intercalation and de-intercalation through the as-prepared  $\text{Li}_4\text{Ti}_5\text{O}_{12}$ . Above results then highly promise the application of rutile  $\text{TiO}_2$  in the synthesis of high performance  $\text{Li}_4\text{Ti}_5\text{O}_{12}$  as lithium battery anode by simple acid treatment in combination with cellulose-assisted combustion synthesis.

#### 4. Conclusions

With nitric acid treated rutile  $\text{TiO}_2$  as the titanium source, phase-pure  $\text{Li}_4\text{Ti}_5\text{O}_{12}$  anode powders were synthesized by a cellulose-assisted combustion process at a reduced temperature of  $800^\circ\text{C}$  for 5 h calcination, more than  $150^\circ\text{C}$  lower than that synthesized by standard solid-state reaction. Besides the contribution from the cellulose-assisted combustion synthesis, the decrease in synthesis temperature was also benefited from the nitric acid treatment of the rutile  $\text{TiO}_2$ , which improved the kinetics of rutile  $\text{TiO}_2$ , and then facilitated the phase reaction to form  $\text{Li}_4\text{Ti}_5\text{O}_{12}$ . The as-prepared  $\text{Li}_4\text{Ti}_5\text{O}_{12}$  sample delivered a capacity of  $\sim 175\text{ mAh g}^{-1}$  at 1 C rate which near the theoretical value, and even reached  $\sim 100\text{ mAh g}^{-1}$  at a high discharge rate of 10 C with high cycling stability. Such

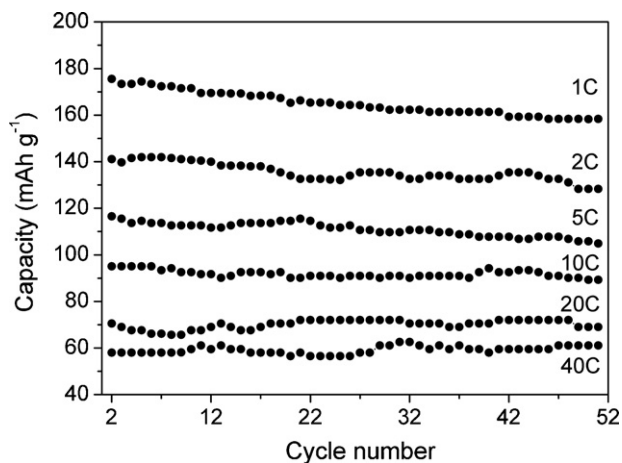


**Fig. 4.** Cycling performance at different discharge rates of the  $\text{Li}_4\text{Ti}_5\text{O}_{12}$  prepared by the cellulose-assisted combustion process and further calcined at  $800^\circ\text{C}$  for 5 h with acid treated rutile  $\text{TiO}_2$  as reactant with the cut-off voltage from 1 to 3 V.

good electrochemical performance for as-synthesized  $\text{Li}_4\text{Ti}_5\text{O}_{12}$  is likely associated with the increased surface area due to the reduced calcination temperature.

### Acknowledgements

This work was supported by National Basic Research Program of China under contract No. 2007CB209704. Dr. Zongping Shao also acknowledges the financial support from Chinese Ministry of Education via the Program for Changjiang Scholars and Innovative Research Team in University (No. IRT0732).

### References

- [1] J.M. Tarascon, M. Armand, *Nature* 414 (2001) 359–367.
- [2] K. Nagajima, Y. Nishi, in: T. Osaka, M. Datta (Eds.), *Energy Storage Systems for Electronics*, Gordon and Breach Science Publisher, Singapore, 2000, p. 109, (Chapter 5).
- [3] K. Sawai, Y. Iwakoshi, T. Ohzuku, *Solid State Ionics* 69 (1994) 273–283.
- [4] D. Aurbach, E. Zinigrad, Y. Cohen, H. Teller, *Solid State Ionics* 148 (2002) 405–416.
- [5] R. Dominko, E. Baudrin, P. Umek, D. Arčon, M. Gaberščeka, J. Jamnik, *Electrochem. Commun.* 8 (2006) 673–677.
- [6] J. Shu, *Electrochim. Acta* 10 (2009) 2869–2876.
- [7] P.P. Prosini, R. Mancini, L. Petrucci, V. Contini, P. Villano, *Solid State Ionics* 144 (2001) 185–192.
- [8] K Zaghib, M. Simoneau, M. Armand, M. Gauthier, *J. Power Sources* 81–82 (1999) 300–305.
- [9] E.M. Sorensen, S.J. Barry, H.K. Jung, J.R. Rondinelli, J.T. Vaughey, K.R. Poeppelmeier, *Chem. Mater.* 18 (2006) 482–489.
- [10] S. Scharner, W. Weppner, P.S. Beurmann, *J. Electrochem. Soc.* 146 (1999) 857–861.
- [11] T. Ohzuku, A. Ueda, N. Yamamoto, *J. Electrochem. Soc.* 142 (1995) 1431–1435.
- [12] A.D. Pasquier, I. Plitz, S. Menocal, G. Amatucci, *J. Power Sources* 115 (2003) 171–178.
- [13] L. Cheng, X.L. Li, H.J. Liu, H.M. Xiong, P.W. Zhang, Y.Y. Xia, *J. Electrochem. Soc.* 154 (2007) A692–A697.
- [14] G.J. Wang, J. Gao, L.J. Fu, N.H. Zhu, Y.P. Wu, T. Takamura, *J. Power Sources* 174 (2007) 1109–1112.
- [15] T. Yuan, R. Cai, K. Wang, R. Ran, S.M. Liu, Z.P. Shao, *Ceram. Int.* 35 (2009) 1757–1768.
- [16] L. Kavan, M. Grätzel, *Electrochem. Solid-State Lett.* 5 (2002) A39–A42.
- [17] D.H. Kim, Y.S. Ahn, J. Kim, *Electrochem. Commun.* 7 (2005) 1340–1344.
- [18] C.M. Shen, X.G. Zhang, Y.K. Zhou, H.L. Li, *Mater. Chem. Phys.* 78 (2003) 437–441.
- [19] Y.H. Rho, K. Kanamura, *J. Solid State Chem.* 177 (2004) 2094–2100.
- [20] Y.J. Hao, Q.Y. Lai, Z.H. Xu, X.Q. Liu, X.Y. Ji, *Solid State Ionics* 176 (2005) 1201–1206.
- [21] M. Venkateswarlu, C.H. Chen, J.S. Do, C.W. Lin, T.C. Chou, B.J. Hwang, *J. Power Sources* 146 (2005) 204–208.
- [22] B.Z. Christiansen, K. West, T. Jacobsen, S. Atlung, *Solid State Ionics* 28–30 (1988) 1176–1182.
- [23] W.J. Macklin, R.J. Neat, *Solid State Ionics* 53–56 (1992) 694–700.
- [24] D.W. Murphy, F.J.D. Salvo, J.N. Carides, J.V. Waszczak, *Mater. Res. Bull.* 13 (1978) 1395–1402.
- [25] S.H. Huang, Z.Y. Wen, X.J. Zhu, Z.X. Lin, *J. Electrochem. Soc.* 152 (1) (2005) A186–A190.
- [26] S.H. Huang, Z.Y. Wen, X.J. Zhu, Z.H. Gu, *Electrochem. Commun.* 6 (2004) 1093–1097.
- [27] T. Yuan, K. Wang, R. Cai, R. Ran, Z.P. Shao, *J. Alloys Compd.* 477 (2009) 665–672.
- [28] H. Ge, N. Li, D.Y. Li, C.S. Dai, D.L. Wang, *Electrochem. Commun.* 10 (2008) 719–722.
- [29] L. Kavan, J. Procházka, T.M. Spittler, M. Kalbáč, M. Zukalová, T. Drezen, M. Grätzel, *J. Electrochem. Soc.* 150 (7) (2003) A1000–A1007.